RSC Advances

ROYAL SOCIETY OF CHEMISTRY

www.rsc.org/advances

RSC Advances

ARTICLE

Surface properties of amphiphilic carbon nanotubes and study of their applicability as basic catalysts

Received 00th January 20xx,
Accepted 00th January 20xx

DOI: 10.1039/x0xx00000x

www.rsc.org/

C. Ramirez-Barria[a,b], A. Guerrero-Ruiz[a,*], E. Castillejos-López[a], I. Rodríguez-Ramos[b], J. Durand[c], J. Volkman[c], P. Serp[c,*]

Amphiphilic hybrid carbon nanotubes (CNTs) containing a hydrophobic undoped section connected to a hydrophilic N-doped segment were synthesized. These amphiphilic hybrid CNTs were characterized by elemental analysis, nitrogen physisorption (BET), thermogravimetric analysis (TGA), transmission electron microscopy (TEM), CO_2 adsorption coupled with microcalorimetry and X-ray photoelectron spectroscopy (XPS). The point of zero charge (PZC) for the different materials was also determined. The presence of basic sites on the surface of N-doped nanotubes is evidenced both from the CO_2 adsorption measurements and the PZC determinations. Their catalytic activity in the aldol condensation of furfural derivatives and acetone was evaluated. The results of the catalytic tests show significant specific activities (amount of reactant converted per gram of solid) when compared with strong basic solutions of NaOH. A clear correlation between the characterization data and the catalytic behavior was found. Furthermore, the selectivity values towards the two main reaction products, C_8 and C_{13} aldol condensation adducts, are close to that of the NaOH solution. All together, these findings suggest these materials might be useful basic catalysts.

Introduction

Carbon materials have been widely employed as solid catalysts, either as active phases or supports. It is well known that the surface properties of carbon materials can be tuned by covalently bonded adatoms.[1] The presence of nitrogen atoms in the basal planes of graphite or graphene layers can change many of their chemical properties. In particular, carbon materials with nitrogen doped graphitic structures displayed surfaces with basic properties.[2] Among carbon materials, carbon nanotubes (CNTs) have become one of the most active research topic in nanoscience and nanotechnology due to their unique electronic, chemical, and mechanical properties.[3] N-doped CNTs have recently been reported as metal-free catalysts in the aerobic oxidation of cyclohexane to adipic acid, the selective oxidation of H_2S, and the oxidative dehydrogenation of propane (ODH).[4–6]

An initial investigation of the Knoevenagel condensation reaction with basic N-doped CNTs, as catalyst, was reported by Van Dommele *et al.*[2] Additionally other catalytic applications, such as transesterification, dehydrogenation and aldol-condensation have also been reported.[7–9] Base catalyzed aldol reactions of oxygenated platform molecules obtained from biomass are amongst the most important recent applications of basic catalysts.[9] The challenge of developing bulk chemicals from biomass or other renewable resources is a field of growing interest.[10–12]

Furfural and its derivatives, such as 5-hydroxymethylfurfural (HMF), are obtained by dehydrating pentoses and hexoses isolated from lignocellulosic biomass.[13] Furfural can react with organic carbonyl compounds such as acetone to form C_8 cross–aldol condensation adducts (FAc, Scheme 1). These products can further condensate with a second molecule of furfural to form C_{13} aldol adducts (F_2Ac, Scheme 1). These adducts are important oxygenated precursors for the synthesis of C_8–C_{15} liquid alkanes obtained after a series of coupled hydrogenation and hydrodeoxygenation reactions.[14]

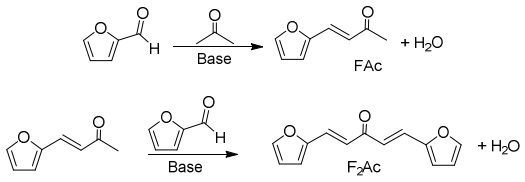

Scheme 1 Representation of the reaction products obtained during the aldol condensation of acetone and furfural

[a] Dpto. Química Inorgánica y Técnica, Facultad de Ciencias UNED, Senda del Rey 9, 28040 Madrid, Spain. E-mail: aguerrero@ccia.uned.es.
[b] Instituto de Catálisis y Petroleoquímica, CSIC, Cantoblanco, Marie Curie 2, 28049 Madrid, Spain.
[c] Laboratoire de Chimie de Coordination, UPR CNRS 8241 composante ENSIACET, Toulouse University, 4 Allée Emile Monso, CS. 44362, Toulouse Cedex 4, France

† Electronic Supplementary Information (ESI) is also available. See DOI: 10.1039/x0xx00000x

Conventional base such as NaOH have been reported as catalyst for the aldol condensation of furfural derivatives and acetone in biphasic systems.[15] However, one of the major drawbacks of these systems is the large amount of homogeneous catalyst required. Alternatively, the development of heterogeneous catalysts based on oxides of alkaline earth metals has been reported for aldol condensation reactions.[16] Hydrotalcites and zeolites (MCM-41) functionalized with amines were also described as basic solid catalysts for aldol condensation reactions.[17,18]

In particular, a variety of mixed oxides have been evaluated as solid base catalysts for the aldol-condensation of furfural and HMF with acetone.[19,20] Thus, in the experiments reported by Faba and coworkers[21] using basic mixed oxides (Mg–Zr, Mg–Al and Ca–Zr), a condensation yield greater than 60% for C13, under mild conditions, was obtained. Resasco *et al*. studied hybrid amphiphilic carbon nanotubes (CNTs) doped with basic oxides (MgO, MgO/Al_2O_3, TiO_2, ZnO, V_2O_5 and $Ce_xZr_{1-x}O_2$).[22] These nanohybrids, when stabilized as emulsions between organic and aqueous phases, display an increased catalytic activity by augmenting the surface area between the two phases. This system has also been shown to catalyze aldol condensation-hydrogenation cascade reactions occurring in the aqueous and organic phases respectively. Recently it has been reported that sequential addition of carbon and nitrogen precursors during the synthesis of CNTs results in the formation of heterojunctions of CNTs and N-CNTs.[23–25] Several studies have been dedicated to establish correlations between the activity and basic properties of carbon materials.[2,26] However, a clear understanding of the surface properties requires well-established methodology to determine and quantify the exposed surface active species.

Herein, the synthesis and characterization of hybrid N-doped CNTs were carried out. Chemical and thermochemical methods, as well as electron microscopy and spectroscopic studies techniques were used to accurately identify the CNTs active surface sites. The catalytic features of these hybrid nanotubes have been investigated for aldol-condensation of furfural and acetone, obtaining relevant catalytic results in terms of activity and selectivity.

Experimental

Synthesis of carbon nanotubes

CNTs were synthesized by a catalytic CVD process in a fluidized bed reactor using ethylene as carbon precursor and acetonitrile as carbon/nitrogen source.[25] An iron catalyst supported on Al_2O_3 was pre-reduced by hydrogen during 30 min at 650 °C and placed in contact with ethylene/H_2 flow (375 mL min^{-1}) at the same temperature, to produce hydrophobic carbon nanotubes or with acetonitrile/Ar/H_2 flow (375 mL min^{-1}) to grow N-CNTs. In order to produce hybrid CNTs, after a first reaction stage, the gas inlet was switched to continue the nanotube growth and produce heterojunctions between undoped and doped nanotubes.

Three CNT samples were produced with (i) ethylene for 30 minutes (E30); (ii) acetonitrile/Ar/H_2 for 30 minutes (A30); and (iii) acetonitrile/Ar/H_2 for 20 minutes followed by ethylene for 10 minutes (A20E10). The produced CNTs were suspended in an aqueous solution of H_2SO_4 (50 vol%) under reflux for 3 h to dissolve the alumina and partially eliminate of exposed metal particles.

Characterization of carbon materials

The CNTs were characterized using transmission electronic microscopy (JEOL JEM-2100F microscope at 200 kV), chemical analysis (C, H and N) using a Perkin-Elmer elemental analyser, and Thermal Analysis (recorded in TG/DTA mode in a TA Instruments SDT Q600) under air. The textural characterization (porosity distribution and BET surface areas, S_{BET}) of the materials was based on N_2 adsorption isotherms, which were obtained using a Micromeritics ASAP 2020 instrument. The samples were also analysed by X-ray photoelectron spectroscopy (XPS) using an Omicron ESCA Probe spectrophotometer, which operated with a non monochromatized Mg K_α source (1253.6 eV).

The amount and strength of the basic sites were determined by CO_2 adsorption using a volumetric equipment described in detail elsewhere.[27] . Successive doses of CO_2 were introduced into the system to titrate the surface of the carbon nanotubes.Prior to the measurements, aliquots (200 mg) of the three synthetised CNTs were pretreated for 2 hours under vacuum at 573 K and outgassed overnight. The adsorption temperature was maintained at 300 K.

To obtain the point of zero charge (PZC), the electrophoretic mobility (μ) vs. pH of the samples was measured in a Zeta Meter 3.0+ at 298 K. The amount of sample used in each point was approximately 100 mg suspended in 100 ml of water. As $\chi . a > 1$ (χ is the reciprocal of Debye length and *a* is the particle radius), the Smoluchowski equation $\mu=\varepsilon_r\varepsilon_0\xi/\eta$ was applied to obtain the zeta potential (ξ). The pH was adjusted adding either HCl or NaOH to the suspensions, which were stabilized for 15 h before μ measurements.

Finally, in order to detect the amphiphilic properties of these materials CNTs samples (30 mg) have been suspended in 10 mL of a biphasic system (1:1, v/v) composed by THF: water (NaCl saturated).

Catalytic test

The aldol condensation of furfural and acetone was performed in a 100 mL stainless steel Parr reactor. The reaction mixture was stirred and heated with a silicone oil bath. In a typical run, the reaction mixture contained 0.1 g of catalyst**,** 1.2 mmol of furfural, 0.6 mmol of acetone and 22 mL of decalin. The reactor temperature was increased to 453 K (reaching a final pressure of 0.25 MPa) and the reaction was allowed to proceed for 15 hours. Thereafter the reaction mixture was cooled down to room temperature and 25 mL of ethyl acetate were added in order to increase the solubility of the products. The samples were filtered and diluted in a stock solution of hexadecane (internal standard) in THF. The analysis was performed with a Clarus 500 gas chromatograph, equipped

with a split/splitless injector, a capillary column (Elite 5 fused silica 30 m, 0.32 mmi.d.) and a flame ionization detector (FID). Quantitative responses were determined using standard calibration mixtures. 1,5-bis(2-furanyl)-1,4-pentadien-3-one (F_2Ac) standard for GC-FID analysis was synthesized as described in the supplementary information and its structure confirmed by ^1H and ^{13}C NMR spectroscopy.
Finally, for comparative purposes catalytic tests using 5 mg and 100 mg of powdered NaOH as catalyst were carried out under the same conditions described (vide supra). Blank experiments with the reactor without any catalyst added, were also performed; the very low conversion values obtained in this experiment was subtracted from conversions achieved in the presence of catalysts.

Results and discussion

Hybrid CNTs synthesis and characterization

TEM images of the E30 samples showed the presence of very regular multi-walled CNTs with an average external diameter of *ca*. 9.7 nm (Fig. 1a). Samples A30 presented a "bamboo-like" structure of N-doped CNTs, with larger diameters (*ca*. 12.9 nm, Fig. 1b). Such structure has been reported in the literature when nitrogen is incorporated into the carbon walls.[28,29] Hybrid samples A20E10 present sections of two different types in the same material: a regular section suggesting the presence of an undoped CNT, and a bamboo-like structure, suggesting the presence of an N-doped CNT (Fig. 1c). Heterojunctions of CNT and N-CNTs, an interesting morphological feature, can also be observed by TEM. CNTs outer diameter size distribution is also provided in Fig. S1.

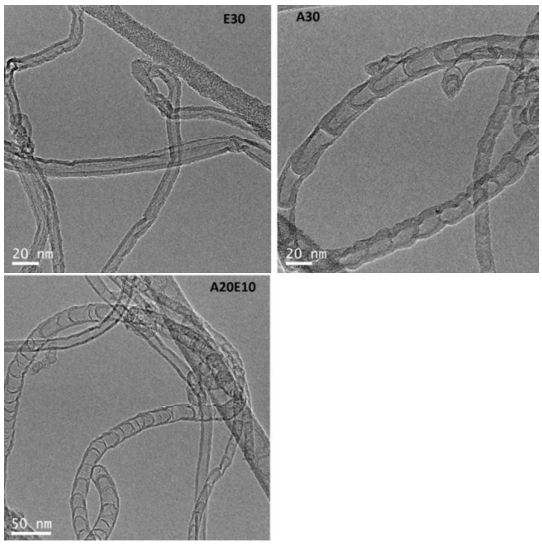

Figure 1. TEM images of CNTs (a) E30; (b) A30; and (c) A20E10

Concerning the material preparation it should be noted that the introduction of nitrogen in the CNT structure decreases the yield of the reaction and increases the tube diameter (Table 1), presumably due to different growth mechanisms.[30]
In addition, the specific surface area (S_{BET}) (Table 1) of E30 is slightly greater than the ones measured for A30 and A20E10. This is coherent with the larger external diameters (measured by TEM) observed for the N-doped samples. Also the narrower CNTs of E30 samples probably favor the formation of bundles.[31] The N_2 adsorption–desorption isotherms of the samples E30, A20E10 and A30 correspond to a type IV nitrogen adsorption isotherms according to the IUPAC classification (Fig. S2 of the supplementary information), which is typical of mesoporous structures.[32]

Table 1. Yield, outer diameter and BET surface area of the produced CNTs.

Sample	Yield ($gCgcat^{-1}$)	Mean diameters (nm)	S_{BET} ($m^2\ g^{-1}$)
E30	5.1	9.7	296
A20E10	2.2	15.1	230
A30	1.1	12.9	227

As far as the chemical composition of these samples is concerned, E30 contains 93.5% of carbon with no nitrogen being detected. Samples A20E10 contain up to 2.0% of N, which further increase to 4.1% for A30 (Table 2).
The thermal reactivity under air of the prepared samples was investigated by TG analyses (Fig. S3). DTG analysis for E30 showed a well-defined peak near 895 K that could be attributed to the oxidation of a well-organized carbon structure. In comparison, sample A30 showed an oxidation temperature of 796 K, which suggests the presence of a more defective and reactive carbon structure. Hybrid CNTs showed two peaks, suggesting the presence of two sections. For the sample A20E10 the main peak at 780 K is related to the N-doped part, and the second contribution at 860 K is related to the carbon sections (Fig. S4). From the measured weight loss, the remaining metal content can be estimated for A30 (~3.2%), A20E10 (~8.6%), and E30 (~10.5%). As iron species are not detected by XPS, the iron is likely to be encapsulated carbide iron structures. The surface charge of carbons is governed by the nature of the surface groups and the pH. PZC, was used to estimate the CNTs surface chemistry (Fig. 2).[1] The PZC values (Table 2) increase as the N content increases from 0 to 4.1%. These results seem to indicate that N-CNTs surfaces present a greater basic character than non-doped CNTs. Since nitrogen adatoms have an additional electron in comparison with carbon atoms, p electron delocalization will occur easily in N-CNTs. This excess of electrons changes the hydrophobicity of the carbon surface. Therefore, electronic density of the N-doped carbon materials increases, which would lead to higher PZC values. As electron-donor properties are related to basicity, the stronger the electron donating is, the greater the basicity.[27]

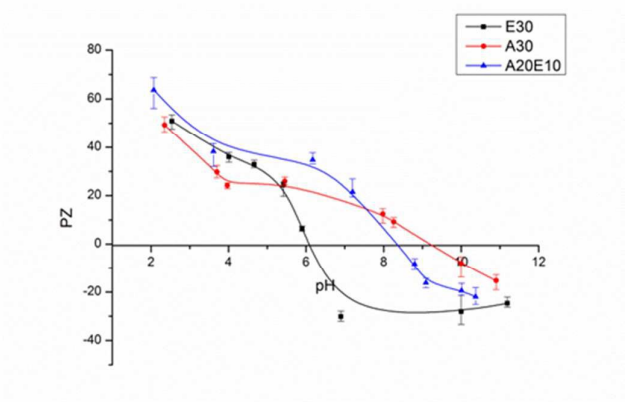

Figure 2. PZC for (a) E30; (b) A30; and (c) A20E10.

Table 2. N content (from microanalysis), isotherm slope, and PZC for the produced CNTs.

Sample	%N EA	Slope CO_2 isotherms	PZC
E30	0	0.38	6.1
A20E10	2.0	1.45	8.2
A30	4.1	1.23	9.1

The chemical composition was also obtained from the characteristic XPS peaks corresponding to C, N and O. These results are shown in Table 3. Nitrogen peak deconvolution (Fig. S4) indicated the presence of four elementary peaks: pyridinic nitrogen (399.5–398.5 eV), pyrrolic nitrogen (400.8–399.8 eV), quaternary nitrogen (403.0–401.0 eV), and NOx groups (404.9–405.6 eV).[9] Of all these species, the pyridinic nitrogen is believed to have the stronger basic character. Accordingly, it is generally assumed that the basicity of carbon catalysts is linked to the amount of pyridinic groups.[2,33]

Table 3. Nitrogen content and contribution species detected by deconvolution of spectra

	E30	A20E10	A30
%C XPS	95.1	91.0	88.1
%O XPS	4.9	4.9	6.3
%N XPS	0.0	4.1	5.7
C/N	-	22.2	15,5
% Pyridinic-N	-	29.7	29.9
% Pyrrolic-N	-	30.6	32.2
% Quaternary-N	-	11.1	17.2
% N-Ox groups	-	28.6	20.7

Volumetric isotherms corresponding to CO_2 adsorption on CNTs samples are depicted in Figure 4. The isotherm slopes increase from non-doped CNTs to N-doped CNTs (Table 2). Since CO_2 possesses a Lewis acidic character, it is expected to be adsorbed on basic sites of the N-CNTs surfaces.[27] The variations in the isotherm slope are thus directly proportional to the amount of surface adsorption sites on the samples. In short, the amount of basis surface sites in our samples follows the order: A20E10>A30>>E30. Unfortunately, the low CO_2 uptakes were not sufficient to measure adsorption heats with enough precision to distinguish between chemisorption and physisorption surface sites.

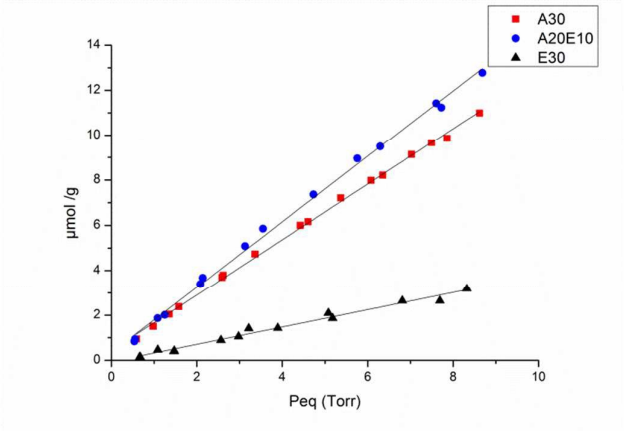

Figure 3. Isotherms of CO_2 adsorption on CNTs samples at 330 K (a) A30; (b) A2E10; and (c) E30

Dispersion test in different biphasic systems such as THF: water (NaCl saturated) showed that after a brief sonication and 6 hours of decantation the best stabilized material at the liquid interphase is A20E10. While E30 tends to be located in the organic phase and A30 remains in the water phase. In the supplementary information an illustrative picture of these differences is provided (Fig. S6).

Aldol condensation of furfural and acetone

The performance of these hybrid CNTs as basic catalyst was tested for the aldol condensation reaction of furfural with acetone. Overall reaction activities and the selectivities toward C_8 (FAc) and C_{13} (F_2Ac) products are given in Table 4.

Materials containing nitrogen groups show significant activity as basic catalysts. Satisfyingly, we obtained a very low specific activity for E30 CNTs, in contrast to N-CNTs. Therefore, the activities of N-CNTs allow us to confirm that basic nitrogen functional groups are involved in this catalytic process. When comparing A30 and A20E10 catalysts, in spite of the higher nitrogen content in the former (Table 2), the specific catalytic activities are very similar. This observation can be rationalized by considering the number of basic nitrogen surface groups (pyridinic species). The pyridinic nitrogen content, as revealed by the XPS study of the N1s peaks, is similar for A20E10 and A30 samples (information shown in Fig. S4 and also reported in Table 3).

For comparison purposes two additional experiments were carried out using NaOH as catalyst (5mg and 100 mg) (*i.e.* homogenous catalytic tests). Interestingly, activities achieved with N-doped samples were higher than those obtained utilizing NaOH as homogeneous catalyst assuming that basicity on the surface of NCNTs is fully related to content of nitrogen. Concerning selectivity, in all cases FAc was identified as the main reaction product. However, selectivity toward F_2Ac

increases for N-doped catalysts when compared to undoped E30 sample.

The present results demonstrate that hybrid CNTs are an attractive material that can be used as metal-free basic catalyst for organic synthetic reactions. Furthermore, their applicability in biphasic media enables heterogeneous catalysis for reaction processes that at present apply homogeneous catalysts, *i.e*. in continuous operations.

Table 4. Catalytic results for aldol condensation reaction

Catalysts	Specific activity (μmol/g)	C Balance	Activity (mol/mol cat)	Sel FAc (%)	Sel F_2Ac (%)
E30	1.4	95.9	-	77	23
A20E10	25.6	98.3	0.089[1]	67	33
A30	27.9	98.4	0.047[1]	63	37
NaOH (5mg)	295.6	98.0	0.012	69	31
NaOH (100 mg)	224.3	97.6	0.009	33	67

1 Atomic density 38 C at/nm^2.

Conclusions

This study provides additional support for our understanding of basic properties of N-doped CNTs. The correlation of the results obtained from different characterization techniques and the catalytic performances demonstrated the potential of the active basic sites exposed in hybrid CNTs as metal free catalysts. The evidence from PZC study suggests that N-doped CNTs surfaces present a higher basic character than non-doped CNTs. Besides, the correlation between the experimental adsorption data and the catalytic results is noteworthy and can be used as a criterion to assess the basicity of the surface.

Catalytic tests for the hybrid CNTs (A20E10 sample) in the aldol-condensation of furfural and acetone highlight the role of these sites in the base-catalysed reactions, since both the conversion and the selectivity to final products increase for this catalyst.

Additionally, these amphiphilic CNTs can interact with polar and non-polar solvents acting on emulsion formation and stabilization, which can be useful for application in catalytic biphasic processes and tandem reactions. We therefore, expect to be able to utilize these materials in biphasic continuous processes.

Acknowledgements

Carolina Ramirez-Barria gratefully acknowledges financial support by the Erasmus program (UNED-Toulouse University) and a grant for Master study from the Sociedad Española de Catálisis (SECAT). Also the financial support from the Spanish Ministerio de Economía y Competitividad under projects CTQ2014-52956-C3-2-R and CTQ2014-52956-C3-3-R is recognized.

Notes and references

1 *Carbon Materials for Catalysis*; Serp, P., Figueiredo, J. L., Eds.; John Wiley & Sons, Inc: New Jersey, 2008.

2 van Dommele, S.; de Jong, K. P.; Bitter, J. H. *Chem. Commun.* **2006**, *76* (46), 4859–4861.

3 Serp, P.; Machado, B. F. *Nanostructured Carbon Materials for Catalysis*; Royal Society of Chemistry: Cambridge, 2015.

4 Yu, H.; Peng, F.; Tan, J.; Hu, X.; Wang, H.; Yang, J.; Zheng, W. *Angew. Chemie - Int. Ed.* **2011**, *50* (17), 3978–3982.

5 Chizari, K.; Deneuve, A.; Ersen, O.; Florea, I.; Liu, Y.; Edouard, D.; Janowska, I.; Begin, D.; Pham-Huu, C. *ChemSusChem* **2012**, *5* (1), 102–108.

6 Chen, C.; Zhang, J.; Zhang, B.; Yu, C.; Peng, F.; Su, D. *Chem. Commun.* **2013**, *49* (207890), 8151–8553.

7 Villa, A.; Tessonnier, J.-P.; Majoulet, O.; Su, D.; Schlögl, R. *ChemSusChem* **2010**, *3* (2), 241–245.

8 Asedegbega-Nieto, E.; Perez-Cadenas, M.; Morales, M. V.; Bachiller-Baeza, B.; Gallegos-Suarez, E.; Rodriguez-Ramos, I.; Guerrero-Ruiz, A. *Diam. Relat. Mater.* **2014**, *44*, 26–32.

9 Faba, L.; Criado, Y. A.; Gallegos-Suarez, E.; Pérez-Cadenas, M.; Díaz, E.; Rodriguez-Ramos, I.; Guerrero-Ruiz, A.; Ordóñez, S. *Appl. Catal. A Gen.* **2013**, *458*, 155–161.

10 Climent, M. J.; Corma, A.; Iborra, S. *Green Chem.* **2014**, *16* (2), 516–547.

11 Sheldon, R. A. *Green Chem.* **2014**, *16* (3), 950–963.

12 Gallezot, P. *Chem. Soc. Rev.* **2012**, *41* (4), 1538–1558.

13 Perego, C.; Ricci, M. *Catal. Sci. Technol.* **2012**, *2* (9), 1776.

14 Huber, G. W.; Chheda, J. N.; Barrett, C. J.; Dumesic, J. A. *Science* **2005**, *308* (5727), 1446–1450.

15 West, R. M.; Liu, Z. Y.; Peter, M.; Dumesic, J. A. *ChemSusChem* **2008**, *1* (5), 417–424.

16 Di Cosimo, J. I.; Díez, V. K.; Apesteguía, C. R. *Appl. Catal. A Gen.* **1996**, *137* (1), 149–166.

17 Climent, M. J.; Corma, A.; Iborra, S.; Epping, K.; Velty, A. *J. Catal.* **2004**, *225* (2), 316–326.

18 Choudary, B. M.; Kantam, M. L.; Sreekanth, P.; Bandopadhyay, T.; Figueras, F.; Tuel, A. *J. Mol. Catal. A Chem.* **1999**, *142* (3), 361–365.

19 Barrett, C. J.; Chheda, J. N.; Huber, G. W.; Dumesic, J. A. *Appl. Catal. B Environ.* **2006**, *66* (1-2), 111–118.

20 Chheda, J. N.; Dumesic, J. A. *Catal. Today* **2007**, *123* (1-4),

59–70.

21 Faba, L.; Díaz, E.; Ordóñez, S. *Appl. Catal. B Environ.* **2012**, *113-114*, 201–211.

22 Zapata, P. A.; Faria, J.; Pilar Ruiz, M.; Resasco, D. E. *Top. Catal.* **2012**, *55*, 38–52.

23 Cao, Y.; Liu, B. T.; Jiao, Q. Z.; Zhao, Y. *South African J. Chem. Tydskr. Vir Chemie* **2011**, *64*, 67–70.

24 Tian, G.-L.; Zhao, M.-Q.; Zhang, Q.; Huang, J.-Q.; Wei, F. *Carbon* **2012**, *50* (14), 5323–5330.

25 Purceno, A. D.; Machado, B. F.; Teixeira, A. P.; Medeiros, T. V; Benyounes, A.; Beausoleil, J.; Menezes, H. C.; Cardeal, Z. L.; Lago, R. M.; Serp, P. *Nanoscale* **2015**, *7* (1), 294–300.

26 Fujita, S.; Katagiri, A.; Watanabe, H.; Asano, S.; Yoshida, H.; Arai, M. *ChemCatChem* **2015**, *7* (18), 2965–2970.

27 Bachiller-Baeza, B.; Rodriguez-Ramos, I.; Guerrero-Ruiz, A. *Langmuir* **1998**, *14* (14), 3556–3564.

28 Gong, K.; Du, F.; Xia, Z.; Durstock, M.; Dai, L. *Science* **2009**, *323* (5915) 760–764.

29 García-García, F. R.; Álvarez-Rodríguez, J.; Rodriguez-Ramos, I.; Guerrero-Ruiz, A. *Carbon* **2010**, *48* (1), 267–276.

30 O'Byrne, J. P.; Li, Z.; Jones, S. L. T.; Fleming, P. G.; Larsson, J. A.; Morris, M. A.; Holmes, J. D. *Chemphyschem* **2011**, *12* (16), 2995–3001.

31 Peigney, A.; Laurent, C.; Flahaut, E.; Bacsa, R. R.; Rousset, A. *Carbon N. Y.* **2001**, *39* (4), 507–514.

32 Thommes, M.; Kaneko, K.; Neimark, A. V.; Olivier, J. P.; Rodriguez-Reinoso, F.; Rouquerol, J.; Sing, K. S. W. *Pure Appl. Chem.* **2015**, *87* (9-10), 1051–1069.

33 Li, B.; Sun, X.; Su, D. *Phys. Chem. Chem. Phys.* **2015**, *17*, 6691–6694.

34 Kurata H.; Isoda S.; Kobayashi T. *Microsc Microanal Microstruct.* **1995**, 6(4), 405–13.